Polarization of ^{21}Ne by Spin Exchange with Optically Pumped Rb Vapor

T. E. Chupp and K. P. Coulter
Joseph Henry Laboratory of Physics, Princeton University, Princeton, New Jersey 08544
(Received 17 June 1985)

We report investigations of spin exchange between ^{21}Ne nuclei and optically pumped Rb vapor. Polarization of 30% ($\langle K_z \rangle = 0.46$) of 2×10^{19} atoms-cm^{-3} has been achieved with a vapor pressure of 3×10^{14} atoms-cm^{-3} of Rb. This high density of alkali metal can be efficiently optically pumped only when light trapping is suppressed by inclusion of at least 100 Torr of N_2. In addition, we have made the first accurate measurement of the binary-collision spin-exchange rate: $\langle \sigma_{ex} v \rangle = (4.66 \pm 0.28)\times10^{-19}$ cm^3-s^{-1}. Extension of these techniques to ^{3}He has yielded 5% polarization of 2×10^{19} atoms-cm^{-3} in a preliminary experiment.

PACS numbers: 32.80.Bx, 29.25.Kf

The technique of nuclear polarization of noble-gas nuclei by spin exchange with optically pumped alkali-metal vapor was first applied to ^{3}He by Bouchiat, Carver, and Varnum.[1] Other stable, odd-A, noble-gas nuclei including isotopes of the heavier noble gases Xe, Ar, Kr,[2] and ^{21}Ne[3] have also been polarized by this technique. Polarized noble-gas nuclei have applications in experimental investigations of fundamental symmetries such as electric dipole-moment searches[4] and searches for inertial-mass anisotropy,[5] as well as potential as polarized targets for high-energy and nuclear physics.[6,7]

For the heavier noble gases, Kr and Xe, the spin-exchange rates are dominated by the formation of relatively long-lived (lifetime $\tau \geq 10^{-9}$ s) van der Waals molecules,[3] whereas for ^{3}He and ^{21}Ne, there is no evidence that such molecules are important[8] and spin exchange occurs during the binary collision time ($\tau \approx 10^{-12}$ s). The other important factor, the coefficient α, depends on the overlap of the alkali-metal valence-electron wave function with the noble-gas nucleus. Alpha is expected to increase with Z of the noble gas because the spin exchange is dominated by s-wave scattering with respect to the noble-gas nucleus. The probability of spin exchange during a collision is proportional to $(\alpha\tau)^2$ and can be expressed as a spin-exchange cross section, σ_{ex}. Herman[9] has estimated $\sigma_{ex} = 10^{-23}$ cm^2 for Rb-^{21}Ne.

We have investigated polarization of ^{21}Ne nuclei by spin exchange with Rb at alkali-metal densities between 3.6×10^{13} and 4.3×10^{14} alkali-metal atoms-cm^{-3}. At these high alkali-metal densities, efficient optical pumping of the Rb is possible only by effective suppression of light trapping (the scattering of resonant, unpolarized light) by inclusion of N_2 gas. For the work described here, pressures of about 60–120 Torr of N_2 were used. We have observed a qualitative dependence of the ^{21}Ne polarization rate on the N_2 density, indicating that the optimum pressure is greater than 120 Torr. The spin-exchange rate $\langle \sigma_{ex} v \rangle$ has been measured at low alkali-metal density where the Rb polarization is nearly 100%. At high alkali-metal density, the polarization rate combined with $\langle \sigma_{ex} v \rangle$ provides a direct measure of the Rb polarization and thus the effectiveness of light-trapping suppression.

The apparatus used to optically pump the Rb, polarize the ^{21}Ne, and measure the polarization is shown in Fig. 1. Pyrex glass cells, 15 mm in diameter, were filled with a droplet of distilled natural Rb metal, 60–120 Torr of N_2, and 300–700 Torr of Ne which was

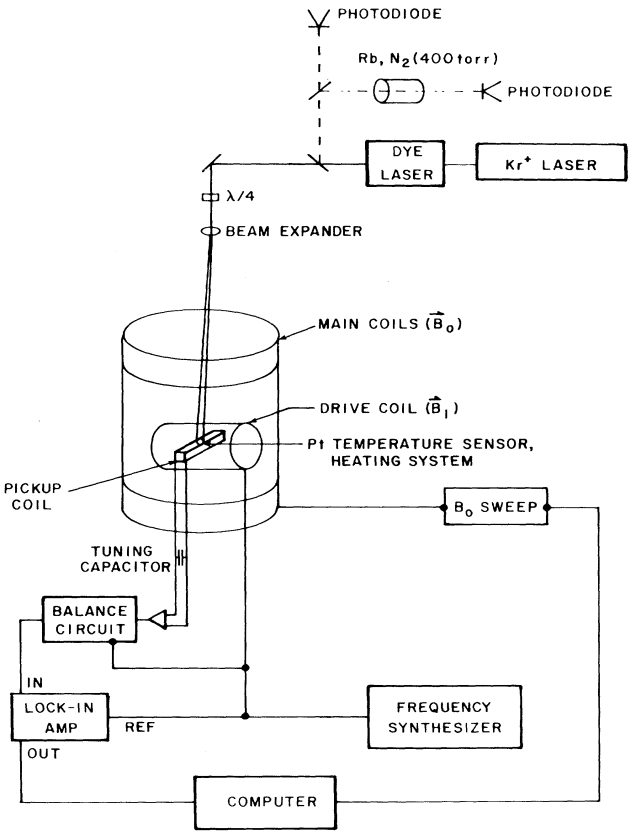

FIG. 1. The apparatus used to optically pump the Rb, polarize the ^{21}Ne, and measure its polarization.

90% ^{21}Ne. A cell was placed in the square-cross-section oven which was fitted with windows for the incident laser light and for viewing the cell. The oven was heated by flowing hot air. The temperature at the coldest part of the cell was measured with a Pt resistor attached to a heat sink which localized the coolest spot and the point where the Rb condensed. The temperature was held constant to 0.2 °C during measurement by a feedback loop which controlled the volume flow of the heated air.

The Rb was optically pumped by D_1 resonant light ($\lambda = 7947$ Å) from a tuned, broadband dye laser with Oxazine 750 dye pumped by a Kr^+ ion laser. The 40-GHz bandwidth of the laser provided a good match to the pressure-broadened resonance-absorption linewidth of 20–30 GHz. The dye-laser output power and frequency were monitored to insure their stability. The light was circularly polarized by a rotatable $\lambda/4$ plate, and expanded to fill the cell. Laser power of 300–400 mW was incident on the cell.

The ^{21}Ne polarization was measured by adiabatic-passage NMR. A tuned circuit consisted of a pickup coil wound onto the oven, in parallel with a capacitor. The circuit was tuned to 120 kHz which is the Larmor precession frequency for ^{21}Ne at 357 G. The 357-G field (B_0) was provided by a pair of thick coils which produced uniformity of better than 1×10^{-3} over the volume of the cell. A 120-kHz oscillating magnetic field ($B_1 = 0.01$ G) was applied at the cell by a pair of Helmholtz drive coils oriented perpendicular to both B_0 and the pickup coil. When B_0 is swept from below resonance to above resonance at a rate of 0.1 G s^{-1}, the ^{21}Ne nuclei flip by adiabatic passage. As the nuclei flip, they precess about B_0 at the Larmor frequency. The precessing magnetization induces a voltage in the pickup coil which was measured by a lock-in amplifier. A balance circuit nulls the background due to eddy-current coupling of the driving field. The experiment is controlled by a microcomputer which drives the magnetic-field sweep and digitizes the lock-in output.

Figure 2 shows the signal produced when the main field is swept twice up and down through the resonance. Some polarization is lost during adiabatic passage because of transverse relaxation of the nuclei as they flip. Two cycles are used to measure this loss which is less than 4%. The signal size, given by the maximum height of the signal above the background, is converted to a vector polarization $\langle K_z \rangle$ by comparison to signals from protons in water for which the polarization and density are known. The proton NMR signals were obtained with identical glass cells in the same apparatus at the same frequency but at 28 G. A correction was applied to account for the difference in magnetic field inhomogeneity which was assumed to be proportional to B_0.

For ^{21}Ne, the buildup of nuclear polarization is described by four coupled differential equations of the form $\dot{\rho}(m_k) = \sum_l R_{k,l}\rho(m_l)$, where $\rho(m_k)$ is the probability that the state m_k is populated. The matrix $R_{k,l}$ is constructed from Fig. 3 which shows the rate constants for transitions among the projections of nuclear spin. For example,

$$R_{-3/2,-3/2} = -\tfrac{6}{5}\gamma\rho_{\mathrm{Rb}}(+\tfrac{1}{2}) - \tfrac{3}{2}\Gamma_1 - \tfrac{1}{4}\Gamma_2 - \tfrac{1}{4}\Gamma_2,$$

and

$$R_{-3/2,-1/2} = \tfrac{6}{5}\gamma\rho_{\mathrm{Rb}}(-\tfrac{1}{2}) + \tfrac{3}{2}\Gamma_1 + \tfrac{1}{4}\Gamma_2.$$

$\rho_{\mathrm{Rb}}(\pm\frac{1}{2})$ is the probability that the Rb valence electron is in the state $m_j = \pm\frac{1}{2}$. γ is defined as the polar-

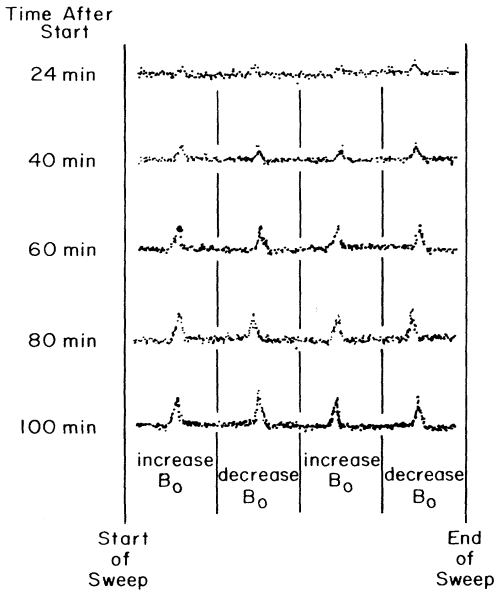

FIG. 2. Raw data for polarization buildup taken at approximately 20-min intervals at 130 °C. Four successive adiabatic-passage flips are used to insure that there is no measurable loss of polarization and to return the ^{21}Ne nuclei to the original orientation.

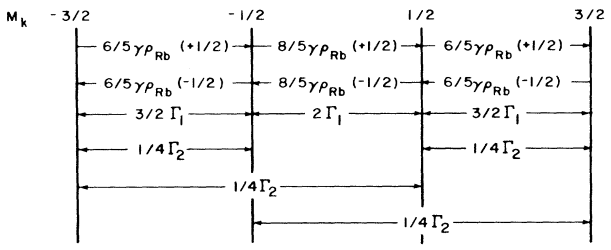

FIG. 3. Schematic illustration of the spin-exchange and relaxation couplings among the Zeeman levels of an $I = \frac{3}{2}$ nucleus and the decay rates for the dipole, quadrupole, and octupole moments of the nuclear polarization with no Rb polarization.

ization rate, $\langle \dot{K}_z \rangle$, when $\langle K_z \rangle = 0$ and the Rb is completely polarized [$\rho_{Rb}(+\frac{1}{2}) = 1$ and $\rho_{Rb}(-\frac{1}{2}) = 0$]. Γ_1 and Γ_2 are relaxation rates due respectively to magnetic dipole and electric quadrupole interactions; relaxation due to octupole interactions has been neglected. The four coupled differential equations reduce to three because the sum of the probabilities $\rho(m_k)$ is constant. Thus polarization buildup is characterized by the sum of three exponentials. With the laser off, the Rb is unpolarized and $\rho_{Rb}(+\frac{1}{2}) = \rho_{Rb}(-\frac{1}{2}) = \frac{1}{2}$. In this case, the polarization decays exponentially with the rate constant $\Gamma = \frac{2}{5}\gamma + \Gamma_1 + \frac{1}{2}\Gamma_2$ and $\langle \dot{K}_z \rangle = -\Gamma \langle K_z \rangle$.

The buildup of ^{21}Ne polarization during optical pumping and the decay of the polarization with the laser off (no Rb polarization) were measured at approximately 20-min intervals as shown in Fig. 2. Measurements were made at cell temperatures of 130, 148, 168, and 180 °C. The data were fitted by the χ^2-minimization technique with uncertainties given by the contributions from NMR signal height, the calibration with proton NMR, and the loss during adiabatic passage. At each temperature, the decay rate was first fitted to determine Γ. The value of Γ was then used to fit the polarization-buildup data to determine γ and Γ_1 with Γ_2 constrained by the value of Γ. Though the best fit is consistent with $\Gamma_2 = 0$, the data are not very sensitive to the relative sizes of Γ_1 and Γ_2 and do not allow a definite conclusion about the dominant relaxation mechanisms. In order to fit the polarization-buildup data, $\rho_{Rb}(+\frac{1}{2})$ is set equal to 1.0. This is a good assumption at 130 °C, based on the observation that the circularly polarized optical pumping light burned completely through the cell. At higher temperatures and densities, the Rb is not completely polarized and the effective "γ" determined by the fit is in fact a measure of the Rb polarization. The values of χ^2_ν are much less than 1 in all cases.

The results are summarized in Fig. 4 where the Rb density for each temperature is assumed to be that given by Killian.[10] The relaxation rate Γ for unpolarized Rb is shown in Fig. 4(a) to be proportional to [Rb] with a slope of about $\frac{2}{5}$ the value of $\langle \sigma_{ex} v \rangle$ determined by fitting the polarization-buildup data [Fig. 4(b)]. We use the best-fit value of $\gamma = \langle \sigma_{ex} v \rangle$[Rb] at 130 °C where Rb relaxation and light-trapping effects are not sufficiently severe to reduce Rb polarization appreciably below 1, to determine $\langle \sigma_{ex} v \rangle = (4.66 \pm 0.28) \times 10^{-19}$ cm^3-s^{-1}, assuming [Rb] $= 3.6 \times 10^{13}$ at 130 °C. With the average ^{21}Ne velocity at this temperature of 7×10^4 cm-s^{-1}, the effective spin-exchange cross section is $\sigma_{ex} = (6.6 \pm 0.4) \times 10^{-24}$ cm^2. The uncertainties given for $\langle \sigma_{ex} v \rangle$ and σ_{ex} assume that [Rb] is exactly known. Though this is not the case, it is not possible to determine the contribution to these uncertainties from the uncertainty in [Rb]. At higher temperatures, the best-fit value for γ falls below the line with slope $\langle \sigma_{ex} v \rangle$ as expected when the Rb is not completely polarized. In Fig. 4(c), the maximum observed ^{21}Ne polarization for this cell is shown to increase to $\langle K_z \rangle = 0.46$ and then fall off at Rb density above 3×10^{14} atoms-cm^{-3}.

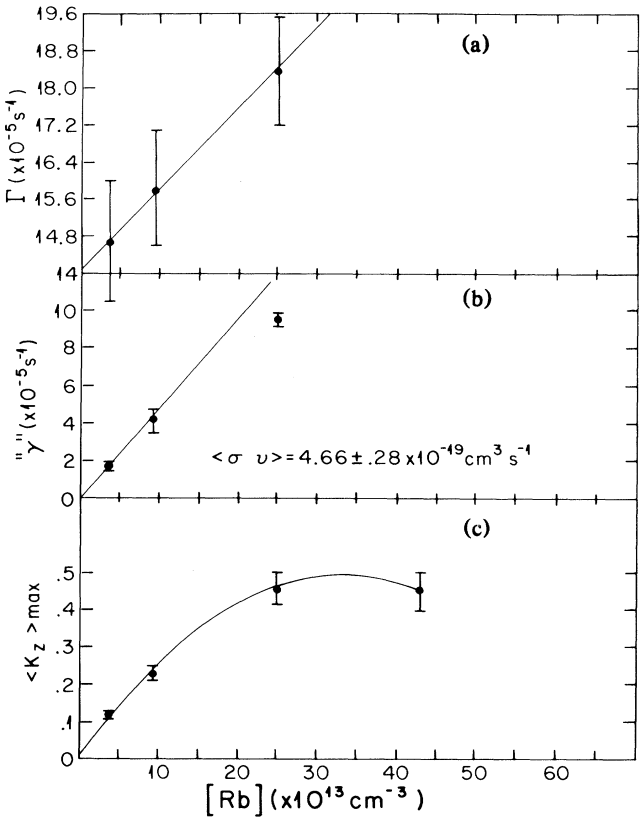

FIG. 4. Summary of results: (a) Γ, the total relaxation rate with unpolarized Rb. (b) "γ," the effective spin-exchange rate determined under the assumption ρRb$(+\frac{1}{2}) = 1.0$. (c) The maximum observed $\langle K_z \rangle$. The lines are drawn to guide the eye and the Rb densities assume the temperature dependence given by Killian (Ref. 10).

Spin exchange with high-density, optically pumped alkali-metal vapor promises to provide greater polarization of ^{3}He than was previously anticipated.[1] In a preliminary experiment, 5% polarization of 500 Torr of ^{3}He has been achieved in a Pyrex cell with Rb and 100 Torr of N_2 at 150 °C (Rb density 9×10^{13} atoms-cm^{-3}). As the work with ^{21}Ne indicates, this is certainly not the limit for ^{3}He polarization by this technique.

The high-density limits of optical pumping are of particular interest and the further study of light-trapping suppression can be achieved by use of the ^{3}He or ^{21}Ne polarization rate as a measure of Rb polarization. By setting $\gamma = \langle \sigma_{ex} v \rangle$ [Rb], Rb polarization can be fitted as a parameter to determine its dependence

on the species and density of buffer gases.

The authors wish to acknowledge and express gratitude to Professor W. Happer and to Professor A. B. McDonald for guidance and many educational discussions. This work was supported in part by National Bureau of Standards Grant No. 60NANB4D0030, National Science Foundation Grant No. PHY83-04977, and U.S. Air Force Office of Scientific Research Grant No. AF0SR-81-0104-C.

[1]M. A. Bouchiat, T. R. Carver, and C. M. Varnum, Phys. Rev. Lett. **5**, 373 (1960).

[2]B. C. Grover, Phys. Rev. A **28**, 2521 (1983).

[3]W. Happer, E. Miron, S. Schaefer, D. Schreiber, W. A. van Wijngaarden, and X. Zeng, Phys. Rev. A **29**, 3092 (1984), and references cited therein.

[4]L. I. Schiff, Phys. Rev. **132**, 2194 (1963); T. G. Vold, F. J. Rabb, B. Heckel, and E. N. Fortson, Phys. Rev. Lett. **52**, 2229 (1984).

[5]T. E. Chupp, "A Search for Local Lorentz Invariance Using Polarized ^{21}Ne Nuclei" (unpublished).

[6]T. E. Chupp, W. Happer, and A. B. McDonald, in *Proceedings of the Workshop on Polarized Targets in Storage Rings, Argonne, Illinois, 1984* (Argonne National Laboratory, Argonne, Ill., 1984), ANL-84-50, p. 177.

[7]A. Bernstein, in Proceedings of the Workshop on Polarized ^{3}He, Princeton, New Jersey, 1984 (American Institute of Physics, New York, to be published).

[8]W. Happer, Phys. Rev. A **31**, 4020 (1985).

[9]R. M. Herman, Phys. Rev. **137**, 1062 (1965).

[10]T. J. Killian, Phys. Rev. **27**, 578 (1926).